Inorganica Chimica Acta 363 (2010) 1469–1478

Contents lists available at ScienceDirect

Inorganica Chimica Acta

journal homepage: www.elsevier.com/locate/ica

Palladium(II) oxalato complexes involving N6-(benzyl)-9-isopropyladenine-based N-donor carrier ligands: Synthesis, general properties, ^{1}H, ^{13}C and $^{15}N\{^{1}H\}$ NMR characterization and *in vitro* cytotoxicity

Pavel Štarha, Igor Popa, Zdeněk Trávníček *

Department of Inorganic Chemistry, Faculty of Science, Palacký University, Tř. 17. listopadu 12, CZ-771 46 Olomouc, Czech Republic

ARTICLE INFO

Article history:
Received 7 December 2009
Received in revised form 15 January 2010
Accepted 22 January 2010
Available online 29 January 2010

Keywords:
Palladium(II) complexes
Oxalate
Adenine derivatives
CDK inhibitors
In vitro cytotoxicity

ABSTRACT

Reactions of potassium bis(oxalato)palladate dihydrate, $K_2[Pd(ox)_2]\cdot 2H_2O$, with two molar equivalents of N6-(benzyl)-9-isopropyladenine-based organic molecules (L_{1-7}), i.e. 2-chloro-N6-(2-methoxybenzyl)-9-isopropyladenine (L_1), 2-chloro-N6-(3-methoxybenzyl)-9-isopropyladenine (L_2), 2-chloro-N6-(3,5-dimethoxybenzyl)-9-isopropyladenine (L_3), 2-(1-ethyl-2-hydroxyethylamino)-N6-(benzyl)-9-isopropyladenine (L_4), 2-(1-ethyl-2-hydroxyethylamino)-N6-(2-methoxybenzyl)-9-isopropyladenine (L_5), 2-(1-ethyl-2-hydroxyethylamino)-N6-(3-methoxybenzyl)-9-isopropyladenine (L_6) and 2-(1-ethyl-2-hydroxyethylamino)-N6-(4-methoxybenzyl)-9-isopropyladenine (L_7), provided a series of seven palladium(II) oxalato (ox) complexes of the general formula $[Pd(ox)(L_{1-7})_2]\cdot nH_2O$ (**1**–**7**; $n = 0$ for **4**, **5** and **7**, ¾ for **1** and **2**, 1 for **6**, and 3 for **3**). The compounds were characterized by elemental analysis, IR, Raman, ^{1}H, ^{13}C and $^{15}N\{^{1}H\}$ NMR spectroscopy, ESI+ mass spectrometry, molar conductivity and TG/DTA thermal analysis. The geometry of $[Pd(ox)(L_2)_2]$ (**2**) was optimized on the B3LYP/6-311G*/LANL2DZ level of theory. The complexes **4**–**7** represent the first palladium(II) oxalato complexes with a PdN_2O_2 donor set, which involve highly potent purine-based cyclin-dependent kinase (CDK) inhibitors (L_{4-7}) as carrier N-donor ligands. The selected complexes **1**, **3**–**5** and **7** were tested by an MTT assay for their *in vitro* cytotoxic activity against human osteosarcoma (HOS) cancer cell line. The highest activity was found for the complexes **5** ($IC_{50} = 34.9$ μM) and **7** ($IC_{50} = 39.2$ μM).

1. Introduction

The plant hormone N6-(benzyl)adenine [6-(benzylamino)-purine] [1] and its derivatives were found to be suitable N-donor ligands of transition metal complexes. In the field of palladium(II) complexes, the *cis*-$[PdCl_2(L)_2]$, *trans*-$[PdCl_2(L)_2]$, $[PdCl_3(L^+)]$, $[PdCl_2(H_2O)(L)]$, $[PdCl(H_2O)_2(L^-)]$ and $[Pd(ox)(L)_2]$ types of compounds were prepared in our laboratory (see lit. [2–5] and the reference cited therein), where L, L^+ and L^- stand for an electroneutral, protonated, and deprotonated N6-(benzyl)adenine derivative, respectively, and ox symbolizes an oxalate dianion.

Talking about the $[Pd(ox)(L)_2]$ compounds in more detail, five complexes with 2-chloro-N6-(benzyl)-9-isopropyladenine, or its analogues with the substituted benzyl group, have recently been published [3]. The molecular and crystal structures of two complexes involving 2-chloro-N6-(4-methoxybenzyl)-9-isopropyladenine (L_I; complex **I**) and 2-chloro-N6-(4-methylbenzyl)-9-isopropyladenine (L_{II}; complex **II**), were determined by a single-crystal X-ray analysis. The mentioned complexes **I** and **II** have the tetra-coordinated central Pd(II) ion which is surrounded by one bidentate-coordinated oxalate dianion and by two monodentate bonded adenine-based molecules (L_I or L_{II}) in a PdN_2O_2 donor set. Moreover, these complexes were tested by a calcein acetoxymethyl (AM) assay for their *in vitro* cytotoxic activity against breast adenocarcinoma (MCF-7) and chronic myelogenous leukaemia (K562) human cancer cell lines. Two of the tested substances showed promising *in vitro* cytotoxicity (IC_{50} values of 6.2 and 6.8 μM), which is higher than those of the commercially used platinum-based anticancer drugs *Cisplatin* ($IC_{50} = 10.9$ μM) and *Oxaliplatin* ($IC_{50} = 18.2$ μM). To our best knowledge, only the $[Pd(ox)(Hoen)_2]\cdot 0.5H_2O$ and $[Pd(ox)(Clen)_2]$ complexes (Hoen = *N,N′*-bis(hydroxyethyl)ethylenediamine, Clen = *N,N′*-bis(chloroethyl)ethylenediamine) [6], besides the above-mentioned $[Pd(ox)(L)_2]$ compounds prepared in our laboratory, were tested for their *in vitro* cytotoxicity within a group of monomeric palladium(II) oxalato complexes, however, these substances were inactive against mice leukaemia (P388) cells. On the other hand, the results obtained in the case of $[Pd(ox)(L)_2]$ showed that this type of complexes represents a promising group of compounds in

* Corresponding author. Tel.: +420 585 634 352; fax: +420 585 634 954.
E-mail address: zdenek.travnicek@upol.cz (Z. Trávníček).

0020-1693/$ - see front matter © 2010 Elsevier B.V. All rights reserved.
doi:10.1016/j.ica.2010.01.035

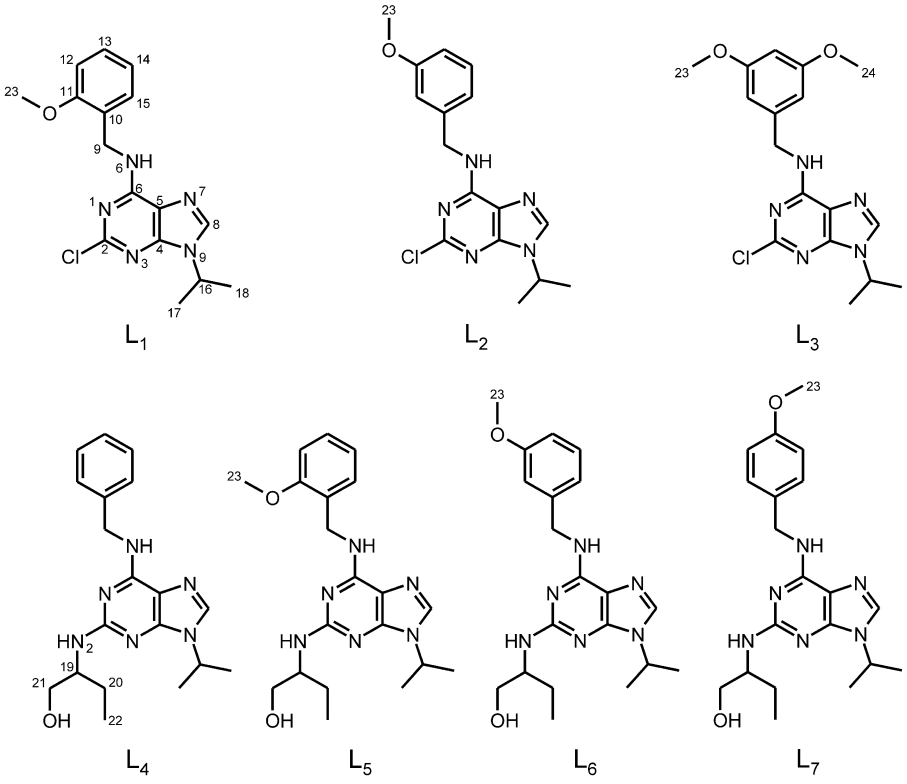

Scheme 1. The derivatives of N6-(benzyl)-9-isoropyladenine (L_{1-7}) used for the preparation of the $[Pd(ox)(L_{1-7})]\cdot nH_2O$ palladium(II) oxalato complexes.

connection with their *in vitro* cytotoxicity. For comparison, other types of biologically active palladium complexes have been reviewed in the literature [2,4].

In this paper, we present results following from our ongoing research of palladium(II) oxalate complexes involving N6-(benzyl)-9-isopropyladenine-based N-donor carrier ligands. We prepared and characterized seven $[Pd(ox)(L)_2]\cdot nH_2O$ complexes of which the compounds **1**–**3** represent analogues of recently reported palladium(II) oxalato complexes [3] varying in the substitution on a benzene ring of the 2-chloro-N6-(benzyl)-9-isopropyladenine moiety (L_{1-3}; see Scheme 1). On the other hand, the complexes **4**–**7** involve differently substituted type of N6-(benzyl)adenine derivatives with 2-amino-1-butanol at the C2 position of a purine ring instead of the chlorine atom, namely 2-(1-ethyl-2-hydroxyethylamino)-N6-(benzyl)-9-isopropyladenine (*Roscovitine*, L_4) [7] and its benzyl-substituted analogues (L_{5-7}; Scheme 1). It is known that *Roscovitine* and its derivatives belong to the group of highly potent cyclin-dependent kinase (CDK) inhibitors, and thus the presented complexes **4**–**7** represent the first palladium(II) oxalato complexes with purine-based CDK inhibitors acting as N-donor carrier ligands.

Based on the above-mentioned statements, we decided to carry out an *in vitro* cytotoxicity screening of the prepared complexes against human osteosarcoma cancer cell line (HOS). The obtained results showed that the complexes **5** and **7**, involving the potent CDK inhibitors, have *in vitro* cytotoxicity comparable with *Cisplatin*, as discussed below. These findings motivated us to evaluate deeply the *in vitro* cytotoxicity of these complexes, and thus, the named palladium(II) oxalato complexes are currently tested against a variety of human cancer cell lines, e.g. MCF-7, lung carcinoma (A549), cervix epithelioid carcinoma (HeLa), ovarian carcinoma (A2780), *Cisplatin*-resistant ovarian carcinoma (A2780*cis*) or malignant melanoma (G-361).

2. Experimental

2.1. Starting materials

Chemicals and solvents were purchased from the commercial sources (Sigma-Aldrich Co., Acros Organics Co., Lachema Co. or Fluka Co.) and they were used as received. Dimethyl sulfoxide (DMSO) was dried using $MgSO_4$.

Potassium bis(oxalato)palladate(II) dihydrate, $K_2[Pd(ox)_2]\cdot 2H_2O$, was prepared from potassium tetrachloropalladate(II), $K_2[PdCl_4]$, as formerly described [3,8]. Syntheses of 2-chloro-N6-(2-methoxybenzyl)-9-isopropyladenine (L_1), 2-chloro-N6-(3-methoxybenzyl)-9-isopropyladenine (L_2), 2-chloro-N6-(3,5-dimethoxybenzyl)-9-isopropyladenine (L_3), 2-(1-ethyl-2-hydroxyethylamino)-N6-(benzyl)-9-isopropyladenine (L_4), 2-(1-ethyl-2-hydroxyethylamino)-N6-(2-methoxybenzyl)-9-isopropyladenine (L_5), 2-(1-ethyl-2-hydroxyethylamino)-N6-(3-methoxybenzyl)-9-isopropyladenine (L_6) and 2-(1-ethyl-2-hydroxyethylamino)-N6-(4-methoxybenzyl)-9-isopropyladenine (L_7) were inspired by several literature sources, and their structures are depicted in Scheme 1 [9–12]. A scheme of the synthetic pathway of the L_{1-7} compounds, as well as the results of IR, Raman and NMR spectroscopies, are given in Appendix A in Supplementary material.

2.2. Preparation of $[Pd(ox)(L_1)_2]\cdot{}^3\!/_4H_2O$ (**1**), $[Pd(ox)(L_2)_2]\cdot{}^3\!/_4H_2O$ (**2**), $[Pd(ox)(L_3)_2]\cdot 3H_2O$ (**3**), $[Pd(ox)(L_4)_2]$ (**4**), $[Pd(ox)(L_5)_2]$ (**5**), $[Pd(ox)(L_6)_2]\cdot H_2O$ (**6**) and $[Pd(ox)(L_7)_2]$ (**7**)

The palladium(II) oxalato complexes **1**–**7** were prepared according to a general synthetic procedure recently published and depicted in Scheme 2 [3]. Briefly, a $K_2[Pd(ox)_2]\cdot 2H_2O$ distilled water solution (15 mL, 40 °C) was mixed together with an acetone solu-

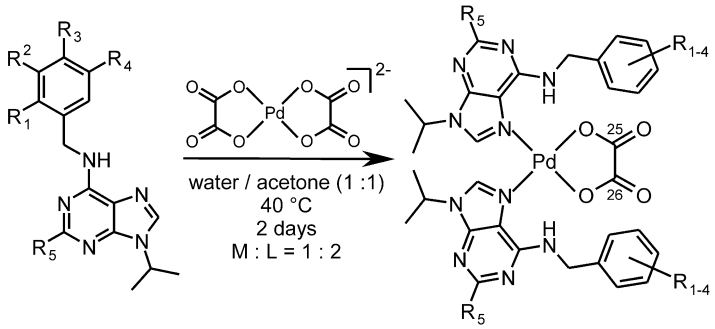

	R_1	R_2	R_3	R_4	R_5
1	OMe	H	H	H	Cl
2	H	OMe	H	H	Cl
3	H	OMe	H	OMe	Cl
4	H	H	H	H	2-amino-1-butanol
5	OMe	H	H	H	2-amino-1-butanol
6	H	OMe	H	H	2-amino-1-butanol
7	H	H	OMe	H	2-amino-1-butanol

Scheme 2. A schematic representation of the preparation pathway of the palladium(II) oxalato complexes **1**–**7**.

tion (15 mL, 25 °C) of the appropriate organic molecule L_{1-7} in a 1:2 molar ratio. The product, which formed during two days of stirring at the temperature of 40 °C, was filtered off, washed with hot (5 mL) and cold (5 mL) distilled water and acetone (5 mL) and dried in the air at 40 °C.

1: Yield: 580 mg (67%). *Anal.* Calc. for $C_{34}H_{36}N_{10}O_6Cl_2Pd\cdot{}^3/_4H_2O$: C, 46.9; H, 4.3; N, 16.1. Found: C, 46.8; H, 4.5; N, 15.9%. m.p. 169–171 °C (decomp.). Λ_M (DMF solution, S cm^2 mol^{-1}): 5.8. ESI+ MS (methanol, *m/z*) $[Pd(ox)(L_1)_3 + H]^+$ 1189.5, $[Pd(ox)(L_1)_2 + K]^+$ 897.0, $[Pd(ox)(L_1)_2 + Na]^+$ 880.9, $[Pd(ox)(L_1)_2 + H]^+$ 858.8, $[Pd(ox)(L_1) + K]^+$ 566.0, $[Pd(ox)(L_1) + Na]^+$ 549.8, $[Pd(ox)(L_1) + H]^+$ 527.9, $[L_1 + H]^+$ 332.1. IR (Nujol; cm^{-1}): 559vs ν(Pd–O), 518 ν(Pd–N). IR (KBr; cm^{-1}): 3130w, 3113w, 3066w ν(C–H)$_{ar}$, 2981w, 2939w, 2836w ν(C–H)$_{al}$; 1707vs, 1671s ν(C=O)$_{ox}$; 1622vs ν(C=N); 1539w, 1491s ν(C=C)$_{ar}$; 1364vs ν(C–O)$_{ox}$; 1242vs ν(C–O)$_{ar}$; 1163w ν(C–Cl); 560w ν(Pd–O). ^{1}H NMR (DMF-d_7, ppm): δ 8.99 (t, 6.2, N^{6}H, 1H), 8.76 (s, C^{8}H, 1H), 7.40 (dd, 7.3, 1.7, C^{15}H, 1H), 7.28 (tt, 7.9, 1.7, C^{14}H, 1H), 7.05 (dd, 8.2, 1.1, C^{12}H, 1H), 6.86 (tt, 7.5, 1.1, C^{13}H, 1H), 4.88 (d, 6.2, C^{9}H, 2H), 4.81 (sp, 6.8, C^{16}H, 1H), 3.94 (s, C^{23}H, 3H), 1.53 (d, 6.8, C^{17}H, C^{18}H, 6H). ^{13}C NMR (DMF-d_7, ppm): δ 165.57 (C^{25}, C^{26}), 157.95 (C^{11}), 155.27 (C^6), 154.25 (C^2), 150.31 (C^4), 143.85 (C^8), 129.02 (C^{13}), 128.72 (C^{15}), 126.66 (C^{10}), 120.98 (C^{14}), 117.31 (C^5), 111.14 (C^{12}), 55.95 (C^{23}), 49.67 (C^{16}), 40.51 (C^9), 21.97 (C^{17}, C^{18}). ^{15}N NMR (DMF-d_7, ppm): δ 230.1 (N^1), 223.0 (N^3), 185.8 (N^9), 147.3 (N^7), 97.5 (N^6).

2: Yield: 590 mg (69%). *Anal.* Calc. for $C_{34}H_{36}N_{10}O_6Cl_2Pd\cdot{}^3/_4H_2O$: C, 46.9; H, 4.3; N, 16.1. Found: C, 46.9; H, 4.4; N, 16.5%. m.p. 178–181 °C (decomp.). Λ_M (DMF solution, S cm^2 mol^{-1}): 0.3. ESI+ MS (methanol, *m/z*): $[Pd(ox)(L_2)_3 + H]^+$ 1189.4, $[Pd(ox)(L_2)_2 + H]^+$ 858.7, $[Pd(ox)(L_2) + H]^+$ 527.8, $[L_2 + H]^+$ 332.2. IR (Nujol; cm^{-1}): 558vs ν(Pd–O), 506s ν(Pd–N). IR (KBr; cm^{-1}): 3114w, 3053w ν(C–H)$_{ar}$, 2977w, 2938w, 2836w ν(C–H)$_{al}$; 1711s, 1675s ν(C=O)$_{ox}$; 1618vs ν(C=N); 1537w, 1488s ν(C=C)$_{ar}$; 1373w ν(C–O)$_{ox}$; 1265s ν(C–O)$_{ar}$; 1165w ν(C–Cl); 559w ν(Pd–O). Raman (cm^{-1}): 3370w ν(N–H); 3139w, 3059w ν(C–H)$_{ar}$; 2990s, 2939s, 2838w ν(C–H)$_{al}$; 1703w, 1659s ν(C=O)$_{ox}$; 1537w, 1485s ν(C=C)$_{ar}$; 1167w ν(C–Cl); 559s ν(Pd–O). ^{1}H NMR (DMF-d_7, ppm): δ 9.22 (t, 6.2, N^{6}H, 1H), 8.77 (s, C^{8}H, 1H), 7.23 (t, 8.0, C^{14}H, 1H), 7.10 (t, 2.2, C^{11}H, 1H), 7.09 (d, 7.8, C^{15}H, 1H), 6.84 (dd, 8.2, 2.6, C^{13}H, 1H), 4.85 (d, 6.2, C^{9}H, 2H), 4.81 (sp, 6.8, C^{16}H, 1H), 3.82 (s, C^{23}H, 3H), 1.53 (d, 6.8, C^{17}H, C^{18}H, 6H). ^{13}C NMR (DMF-d_7, ppm): δ 165.72 (C^{25}, C^{26}), 160.48 (C^{12}), 155.13 (C^2), 154.05 (C^6), 150.32 (C^4), 143.81 (C^8), 140.85 (C^{10}), 130.04 (C^{14}), 120.62 (C^{15}), 117.26 (C^5), 113.91 (C^{11}), 113.31 (C^{13}), 55.50 (C^{23}), 49.64 (C^{16}), 45.19 (C^9), 21.96 (C^{17}, C^{18}). ^{15}N NMR (DMF-d_7, ppm): δ 227.6 (N^1), 217.6 (N^3), 181.5 (N^9), 143.4 (N^7), 97.2 (N^6).

3: Yield: 610 mg (63%). *Anal.* Calc. for $C_{36}H_{40}N_{10}O_8Cl_2Pd\cdot 3H_2O$: C, 44.5; H, 4.8; N, 14.4. Found: C, 44.1; H, 4.7; N, 13.9%. m.p. 176–179 °C (decomp.). Λ_M (DMF solution, S cm^2 mol^{-1}): 0.1. ESI+ MS (methanol, *m/z*): $[Pd(ox)(L_3)_3 + H]^+$ 1279.4, $[Pd(ox)(L_3)_2 + H]^+$ 918.6, $[Pd(ox)(L_3) + K]^+$ 596.8, $[Pd(ox)(L_3) + H]^+$ 557.9, $[L_3 + H]^+$ 362.1. IR (Nujol; cm^{-1}): 560vs ν(Pd–O); 521s ν(Pd–N). IR (KBr; cm^{-1}): 3137w, 3111w, 3057w ν(C–H)$_{ar}$, 2982w, 2941w, 2838w ν(C–H)$_{al}$; 1712vs, 1676s ν(C=O)$_{ox}$; 1619vs ν(C=N); 1539w, 1470s ν(C=C)$_{ar}$; 1378s ν(C–O)$_{ox}$; 1229w ν(C–O)$_{ar}$; 1156s ν(C–Cl); 560w ν(Pd–O); 521w ν(Pd–N). Raman (cm^{-1}): 3333w ν(N–H); 3137w, 3076w, 3014w ν(C–H)$_{ar}$; 2985s, 2945s, 2838w ν(C–H)$_{al}$; 1697s, 1657w ν(C=O)$_{ox}$; 1535w, 1486w ν(C=C)$_{ar}$; 1166w ν(C–Cl); 560s ν(Pd–O); 521w ν(Pd–N). ^{1}H NMR (DMF-d_7, ppm): δ 9.18 (t, 6.2, N^{6}H, 1H), 8.76 (s, C^{8}H, 1H), 6.72 (d, 2.4, C^{11}H, C^{15}H, 2H), 6.41 (t, 2.4, C^{13}H, 1H), 4.82 (d, 6.2, C^{9}H, 2H), 4.79 (sp, 6.8, C^{16}H, 1H), 3.81 (s, C^{23}H, C^{24}H, 6H), 1.53 (d, 6.8, C^{17}H, C^{18}H, 6H). ^{13}C NMR (DMF-d_7, ppm): δ 165.59 (C^{25}, C^{26}), 161.67 (C^{12}, C^{14}), 155.14 (C^6), 154.10 (C^2), 150.36 (C^4), 143.80 (C^8), 141.65 (C^{10}), 117.32 (C^5), 106.48 (C^{11}, C^{15}), 99.75 (C^{13}), 55.66 (C^{23}, C^{24}), 49.64 (C^{16}), 45.39 (C^9), 21.99 (C^{17}, C^{18}). ^{15}N NMR (DMF-d_7, ppm): δ 231.2 (N^1), 223.8 (N^3), 185.8 (N^9), 147.5 (N^7), 100.4 (N^6).

4: Yield: 320 mg (71%). *Anal.* Calc. for $C_{40}H_{52}N_{12}O_6Pd$: C, 53.2; H, 5.8; N, 18.6. Found: C, 52.7, H, 6.1; N, 18.5%. m.p. 164–166 °C (decomp.). Λ_M (DMF solution, S cm^2 mol^{-1}): 0.3. ESI+ MS (methanol, *m/z*): $[Pd(ox)(L_4)_3 + H]^+$ 1257.0, $[Pd(ox)(L_4)_2 + Na]^+$ 925.2, $[Pd(L_4)_2 + H]^+$ 813.1, $[Pd(L_4) + Na]^+$ 571.1, $[Pd(L_4) + H]^+$ 461.2, $[L_4 + H]^+$ 355.3. IR (Nujol; cm^{-1}): 559vs ν(Pd–O); 524vs ν(Pd–N). IR (KBr; cm^{-1}): 3131w, 3062w, 3030w ν(C–H)$_{ar}$, 2965s, 2932s, 2875s ν(C–H)$_{al}$; 1706vs, 1674s ν(C=O)$_{ox}$; 1610vs ν(C=N); 1545vs, 1493vs ν(C=C)$_{ar}$; 1376vs ν(C–O)$_{ox}$; 1058s ν(C–O)$_{al}$; 560w ν(Pd–O); 523w ν(Pd–N). Raman (cm^{-1}): 3148w, 3057vs ν(C–H)$_{ar}$; 2979s, 2935vs, 2877s ν(C–H)$_{al}$; 1692w, ν(C=O)$_{ox}$; 1606vs ν(C–N); 1491s ν(C=C)$_{ar}$; 561w ν(Pd–O). ^{1}H NMR (DMF-d_7, ppm): δ 8.43 (br, N^{6}H, 1H), 8.38 (s, C^{8}H, 1H), 7.50 (dd, 7.2, 1.6, C^{11}H, C^{15}H, 2H), 7.31 (tt, 7.2, 1.6, C^{12}H, C^{14}H, 2H), 7.23 (tt, 7.2, 1.6, C^{13}H, 1H), 6.32 (br, N^{2}H, 1H), 4.80 (d, 6.0, C^{9}H, 2H), 4.70 (m, O^{20}H, 1H), 4.67 (sp, 6.8, C^{16}H, 1H), 3.97 (sx, 6.8, C^{19}H, 1H), 3.66 (sx, 6.8, C^{20}H^a, 1H), 3.59 (sx, C^{20}H^b, 1H), 1.75 (sp, 6.8, C^{21}H^a, 1H), 1.56 (m, C^{21}H^b, 1H), 1.50 (d, 6.8, C^{17}H, C^{18}H, 6H), 0.93 (t, 6.8, C^{22}H, 3H). ^{13}C NMR (DMF-d_7, ppm): δ 166.20 (C^{25}, C^{26}), 160.44 (C^2), 153.50 (C^6), 151.43 (C^4), 140.57 (C^{10}), 139.24 (C^8), 128.80 (C^{12}, C^{14}), 128.32 (C^{11}, C^{15}), 127.21 (C^{13}), 111.84 (C^5), 64.12 (C^{20}), 55.35 (C^{19}), 48.39 (C^{16}), 44.61 (C^9), 24.76 (C^{21}), 21.84 (C^{17}), 21.80 (C^{18}), 10.93 (C^{22}). ^{15}N NMR (DMF-d_7, ppm): δ 199.8 (N^1), 181.0 (N^9), 144.3 (N^7), 96.7 (N^2), 91.6 (N^6).

5: Yield: 240 mg (50%). *Anal.* Calc. for $C_{42}H_{56}N_{12}O_8Pd$: C, 52.4; H, 5.9; N, 17.4. Found: C, 51.9, H, 5.8; N, 17.6%. m.p. 159–160 °C (decomp.). Λ_M (DMF solution, S cm^2 mol^{-1}): 3.0. ESI+ MS (methanol, *m/z*): $[Pd(ox)(L_5)_3 + H]^+$ 1347.2, $[Pd(L_5) + H]^+$ 491.1, $[L_5 + H]^+$ 385.3. IR (Nujol; cm^{-1}): 559vs ν(Pd–O); 527vs ν(Pd–N). IR (KBr; cm^{-1}): 3116w, 3072w ν(C–H)$_{ar}$, 2964w, 2933w, 2875w, 2837w ν(C–H)$_{al}$; 1708s, 1676s ν(C=O)$_{ox}$; 1609vs ν(C=N); 1541s, 1492s

ν(C=C)$_{ar}$; 1371s ν(C–O)$_{ox}$; 1243s ν(C–O)$_{ar}$; 1050w ν(C–O)$_{al}$; 556w ν(Pd–O); 526w ν(Pd–N). Raman (cm^{-1}): 3345w ν(N–H); 3069s ν(C–H)$_{ar}$; 2974s, 2936vs, 2878s, 2842w ν(C–H)$_{al}$; 1705w, 1672w, ν(C=O)$_{ox}$; 1606vs ν(C–N); 1536w, 1491s ν(C=C)$_{ar}$; 1251s ν(C–O)$_{ar}$; 1049 ν(C–O)$_{al}$; 560w ν(Pd–O); 526w ν(Pd–N). ^{1}H NMR (DMF-d_7, ppm): δ 8.34 (s, C^{8}H, 1H), 8.23 (br, N^{6}H, 1H), 7.40 (d, 7.5, C^{15}H, 1H), 7.24 (tt, 7.9, 1.6, C^{13}H, 1H), 7.02 (d, 8.2, C^{12}H, 1H), 6.85 (t, 7.5, C^{14}H, 1H), 6.29 (br, N^{2}H, 1H), 4.80 (d, 7.3, C^{9}H, 2H), 4.70 (br, O^{20}H, 1H), 4.68 (sp, 6.8, C^{16}H, 1H), 3.94 (m, C^{19}H, 1H), 3.91 (s, C^{23}H, 3H), 3.64 (m, C^{20}H^a, 1H), 3.56 (m, C^{20}H^b, 1H), 1.72 (sp, 7.4, C^{21}H^a, 1H), 1.55 (sp, 7.4, C^{21}H^b, 1H), 1.50 (d, 6.8, C^{17}H, C^{18}H, 6H), 0.91 (br, C^{22}H, 3H). ^{13}C NMR (DMF-d_7, ppm): δ 165.94 (C^{25}, C^{26}), 160.49 (C^2), 157.95 (C^{11}), 153.64 (C^6), 151.40 (C^4), 139.28 (C^8), 128.87 (C^{13}), 128.61 (C^{15}), 127.90 (C^{10}), 120.87 (C^{14}), 112.07 (C^5), 110.92 (C^{12}), 64.05 (C^{20}), 55.83 (C^{23}), 55.38 (C^{19}), 48.36 (C^{16}), 39.75 (C^9), 24.78 (C^{21}), 21.86 (C^{17}), 21.82 (C^{18}), 10.96 (C^{22}). ^{15}N NMR (DMF-d_7, ppm): δ 200.0 (N^1), 181.8 (N^9), 180.0 (N^3), 145.4 (N^7), 96.9 (N^2), 89.7 (N^6).

6: Yield: 370 mg (77%). *Anal.* Calc. for $C_{42}H_{56}N_{12}O_8Pd{\cdot}H_2O$: C, 51.4; H, 6.0; N, 17.1. Found: C, 51.0, H, 6.1; N, 17.2%. m.p. 155–158 °C (decomp.). Λ_M (DMF solution, S cm^2 mol^{-1}): 2.4. ESI+ MS (methanol, *m/z*): [Pd(ox)(L$_6$)$_3$ + H]$^+$ 1347.0, [Pd(L$_6$) + H]$^+$ 491.2, [L$_6$ + H]$^+$ 385.3. IR (Nujol; cm^{-1}): 557vs ν(Pd–O); 524vs ν(Pd–N). IR (KBr; cm^{-1}): 3120w ν(C–H)$_{ar}$, 2965w, 2934w, 2875w, 2834w ν(C–H)$_{al}$; 1708s, 1676s ν(C=O)$_{ox}$; 1609vs ν(C=N); 1544s, 1491s ν(C=C)$_{ar}$; 1374s ν(C–O)$_{ox}$; 1265s ν(C–O)$_{ar}$; 1047w ν(C–O)$_{al}$; 558w ν(Pd–O). Raman (cm^{-1}): 3061w ν(C–H)$_{ar}$; 2975s, 2937vs, 2876s, 2833w ν(C–H)$_{al}$; 1701w, 1669w, ν(C=O)$_{ox}$; 1608vs ν(C–N); 1542w, 1488w ν(C=C)$_{ar}$; 1266s ν(C–O)$_{ar}$; 559s ν(Pd–O); 526w ν(Pd–N). ^{1}H NMR (DMF-d_7, ppm): δ 8.46 (br, N^{6}H, 1H), 8.36 (s, C^{8}H, 1H), 7.21 (t, 7.9, C^{14}H, 1H), 7.13 (t, 2.1, C^{11}H, 1H), 7.08 (d, 7.6, C^{15}H, 1H), 6.81 (dd, 8.2, 2.6, C^{13}H, 1H), 6.34 (br, N^{2}H, 1H), 4.82 (br, O^{20}H, 1H), 4.76 (d, 6.8, C^{9}H, 2H), 4.68 (sp, 6.8, C^{16}H, 1H), 3.95 (sx, 5.5, C^{19}H, 1H), 3.80 (s, C^{23}H, 3H), 3.66 (sp, 5.5, C^{20}H^a, 1H), 3.55 (m, C^{20}H^b, 1H), 1.74 (sp, 7.4, C^{21}H^a, 1H), 1.55 (sp, 7.4, C^{21}H^b, 1H), 1.50 (d, 6.8, C^{17}H, C^{18}H, 6H), 0.92 (t, 7.5, C^{22}H, 3H). ^{13}C NMR (DMF-d_7, ppm): δ 166.04 (C^{25}, C^{26}), 160.54 (C^{12}), 160.44 (C^2), 153.53 (C^6), 151.46 (C^4), 142.32 (C^{10}), 139.32 (C^8), 129.85 (C^{14}), 120.60 (C^{15}), 113.67 (C^{11}), 113.11 (C^{13}), 111.87 (C^5), 64.12 (C^{20}), 55.47 (C^{23}), 55.36 (C^{19}), 48.34 (C^{16}), 44.68 (C^9), 24.77 (C^{21}), 21.88 (C^{17}), 21.84 (C^{18}), 10.96 (C^{22}). ^{15}N NMR (DMF-d_7, ppm): δ 199.6 (N^1), 181.1 (N^9), 144.7 (N^7), 96.8 (N^2), 91.7 (N^6).

7: Yield: 320 mg (66%). *Anal.* Calc. for $C_{42}H_{56}N_{12}O_8Pd$: C, 52.4; H, 5.9; N, 17.4. Found: C, 52.2, H, 6.4; N, 17.3%. mp 165–167 °C (decomp.). Λ_M (DMF solution, S cm^2 mol^{-1}): 3.2. ESI+ MS (methanol, *m/z*): [Pd(ox)(L$_7$)$_3$ + H]$^+$ 1347.0, [Pd(L$_7$) + H]$^+$ 491.1, [L$_7$ + H]$^+$ 385.3. IR (Nujol; cm^{-1}): 560vs ν(Pd–O); 522vs ν(Pd–N). IR (KBr; cm^{-1}): 3132w ν(C–H)$_{ar}$, 2964s, 2933s, 2875s, 2835w ν(C–H)$_{al}$; 1707vs, 1675s ν(C=O)$_{ox}$; 1608vs ν(C=N); 1543vs, 1493s ν(C=C)$_{ar}$; 1374vs ν(C–O)$_{ox}$; 1249vs ν(C–O)$_{ar}$; 1057w ν(C–O)$_{al}$; 561w ν(Pd–O); 525w ν(Pd–N). Raman (cm^{-1}): 3335w ν(N–H); 3058s ν(C–H)$_{ar}$; 2976s, 2936vs, 2876s, 2842w ν(C–H)$_{al}$; 1711w, 1672w, ν(C=O)$_{ox}$; 1610vs ν(C–N); 1549w ν(C=C)$_{ar}$; 1255w ν(C–O)$_{ar}$; 561w ν(Pd–O). ^{1}H NMR (DMF-d_7, ppm): δ 8.36 (br, N^{6}H, 1H), 8.33 (s, C^{8}H, 1H), 7.45 (dd, 8.6, 2.0, C^{12}H, C^{14}H, 2H), 6.87 (dd, 8.6, 2.0, C^{11}H, C^{15}H, 2H), 6.35 (br, N^{2}H, 1H), 4.77 (t, 6.0, O^{20}H, 1H), 4.71 (d, 5.5, C^{9}H, 2H), 4.67 (sp, 6.6, C^{16}H, 1H), 3.99 (br, C^{19}H, 1H), 3.78 (s, C^{23}H, 3H), 3.69 (m, C^{20}H^a, 1H), 3.57 (m, C^{20}H^b, 1H), 1.77 (sp, 6.8, 1.5, C^{21}H^a, 1H), 1.58 (sp, 6.8, C^{21}H^b, 1H), 1.49 (d, 6.8, C^{17}H, C^{18}H, 6H), 0.94 (tt, 7.5, 2.5, C^{22}H, 3H). ^{13}C NMR (DMF-d_7, ppm): δ 166.10 (C^{25}, C^{26}), 160.48 (C^2), 159.31 (C^{13}), 153.48 (C^6), 151.42 (C^4), 139.30 (C^8), 132.45 (C^{10}), 129.83 (C^{12}, C^{14}), 114.24 (C^{11}, C^{15}), 111.87 (C^5), 64.19 (C^{20}), 55.48 (C^{23}), 55.40 (C^{19}), 48.42 (C^{16}), 44.14 (C^9), 24.81 (C^{21}), 21.81 (C^{17,18}), 10.97 (C^{22}). ^{15}N NMR (DMF-d_7, ppm): δ 200.0 (N^1), 181.2 (N^9), 144.4 (N^7), 97.3 (N^2), 93.3 (N^6).

2.3. Physical measurements

Elemental analyses (C, H, N) were performed on a Fisons EA-1108 CHNS-O Elemental Analyzer (Thermo Scientific). The yields were calculated and based on palladium. Melting point determinations were performed on a Melting Point B-540 apparatus (Büchi) with 5 °C min^{-1} gradient and the obtained values were uncorrected. Conductivity measurements were carried out on a Cond 340i/SET (WTW) in *N,N′*-dimethylformamide (DMF; 10^{-3} M) solution at the temperature of 25 °C. Infrared spectra were recorded on a Nexus 670 FT-IR (ThermoNicolet) by KBr (400–4000 cm^{-1}) and Nujol (150–600 cm^{-1}) techniques. Raman spectroscopy was performed on an NXR FT-Raman Module (ThermoNicolet) in the 150–3750 cm^{-1} region; the Raman spectrum was not obtained in case of **1** (the sample burnt under laser beam). The reported IR and Raman signal intensities have been defined as w = weak, s = strong and vs = very strong. ^{1}H and ^{13}C spectra and ^{1}H–^{1}H gs-COSY, ^{1}H–^{13}C gs-HMQC, ^{1}H–^{13}C gs-HMBC and ^{1}H–^{15}N gs-HMBC (gs = gradient selected, COSY = correlation spectroscopy, HMQC = Heteronuclear Multiple Quantum Coherence, HMBC = Heteronuclear Multiple Bond Coherence) correlation experiments (DMF-d_7 solutions of L$_{1-7}$ and **1**–**7**) were measured on a Varian 400 MHz NMR device at 400.00 MHz (^{1}H), 100.58 MHz (^{13}C) and 40.53 MHz (^{15}N). Spectra were obtained at natural abundance at 300 K (^{1}H and ^{1}H–^{15}N gs-HMBC also at 340 K) and were calibrated against the signals of tetramethylsilane (an internal standard for ^{1}H and ^{13}C NMR spectra) and against the residual signals of the solvent (an internal reference for ^{15}N adjusted to 104.7 ppm). The splitting of proton resonances in the reported ^{1}H spectra is defined as s = singlet, d = doublet, t = triplet, sx = sextuplet, sp = septuplet, br = broad band, dd = doublet of doublets, tt = triplet of triplets, m = multiplet. Mass spectra (MS) of the methanol solutions of **1**–**7** were obtained using a LCQ Fleet ion trap mass spectrometer by the positive mode electrospray ionization (ESI+) technique (Thermo Scientific). Simultaneous thermogravimetric (TG) and differential thermal (DTA) analyses were carried out using a thermal analyzer Exstar TG/DTA 6200 (Seiko Instruments Inc.). TG/DTA studies were performed in ceramic pans from laboratory temperature to 900 °C with a 2.5 °C min^{-1} temperature gradient in dynamic air atmosphere (100 mL min^{-1}). Geometry of the complex **2** was fully optimized at the B3LYP level with the 6-311G*/LANL2DZ basis set, where the LANL2DZ pseudo-potential was applied for the Pd(II) ion. Theoretical calculations were performed with SPARTAN06 program package [13]. The molecular graphic was drawn by DIAMOND, the structural parameters and calculations were interpreted using the same software [14].

2.4. In vitro cytotoxic activity

In vitro cytotoxicity of the complexes **1**, **3**–**5** and **7** was evaluated by an MTT assay against the human osteosarcoma cancer cell line (HOS); [MTT = 3-(4,5-dimethylthiazol-2-yl)-2,5-diphenyltetrazolium bromide] [15].

The suspension of 2.5 × 10^4 cells/well was stabilized in 96-well microplates in the culture medium enriched by fetal calf serum for 16 h at the temperature of 37 °C in 5% CO_2 atmosphere. The tested complexes were dissolved in DMF up to concentration of 50 μM, and then diluted with the cell culture medium to the final DMF concentration of 0.1%. This mixture was added to microplates with the cancer cells instead of the above-mentioned culture medium. The cancer cells were incubated for the period of 24 h. After this period, the cells were washed with sterile phosphate buffer saline (PBS), and 100 μL of MTT (0.3 mg mL^{-1}) were poured in. The medium including the complexes was removed after 2 h. 100 μL of DMSO with 1% NH_3 were added to dissolve the purple formazane, whose absorbance was measured at 630 nm (an automatic

microplate ELISA reader). The obtained results are discussed as IC_{50} values.

3. Results and discussion

3.1. General features

The palladium(II) oxalato complexes of the general composition $[Pd(ox)(L_{1-7})_2]\cdot nH_2O$ (**1**–**7**; n = 0 for **4**, **5** and **7**, ¾ for **1** and **2**, 1 for **6** and 3 for **3**) have been prepared by a one-step synthesis using the reaction of $K_2[Pd(ox)_2]\cdot 2H_2O$ with two molar equivalents of the appropriate N6-(benzyl)-9-isopropyladenine-based organic molecule (L_{1-7}; specified in Section 2.1 and Scheme 1). The pale yellow powder complexes **1**–**7** were isolated after two days of stirring at 40 °C by filtration from the reaction mixture (Scheme 2).

The complexes **1**–**7** were determined to be non-electrolytes, since the molar conductivity values of their 10^{-3} M DMF solutions ranged from 0.1 to 5.8 S cm^2 mol^{-1}, and these values are typical for non-electrolytes in DMF [16].

The prepared palladium(II) oxalato complexes **1**–**7** are well soluble in various solvents (e.g. DMF, DMSO, chloroform, ethanol, methanol, acetone) and less soluble in water. However, the attempts to prepare crystals suitable for a single-crystal X-ray analysis have been unsuccessful to date in all the above-mentioned solvents or their combinations. That is why the composition and structure of complexes **1**–**7** were deduced from the obtained results of physical techniques (mainly from NMR and mass spectra) and based on similarity with the previously published $[Pd(ox)(L_I)_2]$ (**I**) and $[Pd(ox)(L_{II})_2]\cdot L_{II}\cdot Me_2CO$ (**II**) complexes whose structures were determined by a single-crystal X-ray analysis; L_I = 2-chloro-N6-(4-methoxybenzyl)-9-isopropyladenine and L_{II} = 2-chloro-N6-(4-methylbenzyl)-9-isopropyladenine [3]. For the lack of single crystals suitable for a crystallographic study, the geometry of the complex **2** was optimized using DFT calculations (see Section 3.5).

3.2. IR and Raman spectroscopy

The title $[Pd(ox)(L_{1-7})_2]\cdot nH_2O$ complexes (**1**–**7**) involve two types of ligands, i.e. the N-donor ligands (L_{1-7}) derived from N6-(benzyl)-9-isopropyladenine, and O-donor bidentate-coordinated oxalate dianion (ox). Characteristic vibrations of both ligand types were unambiguously detected in the IR (150–4000 cm^{-1}) and Raman (150–3750 cm^{-1}) spectra.

The L_{1-7} organic molecules coordinated to the central Pd(II) ion in the complexes **1**–**7** showed characteristic and the most intensive ν(C=N) bands at 1608–1622 cm^{-1} [17,18]. It should be pointed out, that the maxima values differ between the groups of complexes **1**–**3** (1618–1622 cm^{-1}) and **4**–**7** (1608–1610 cm^{-1}), which may be connected with a different substitution of N6-(benzyl)-9-isopropyladenine skeleton at the C2 position. The peaks of the $\nu(C–H)_{ar}$ and $\nu(C–H)_{al}$ vibrations were detected at 3030–3137 and 2834–2982 cm^{-1}, respectively [17–19]. The $\nu(C{=}C)_{ar}$ bands showed two maxima at ~1470 and ~1545 cm^{-1}. The bands observed in the 1229–1265 cm^{-1} region are assignable to the $\nu(C–O)_{ar}$ vibration of the methoxy substituent of a benzyl group (it was not found in case of **4**, which does not have the methoxy-substituted benzene ring). The presence of the ν(C–Cl) (for **1**–**3**) and $\nu(C–O)_{al}$ (for **4**–**7**) vibrations at ~1050 and ~1160 cm^{-1}, respectively, is a consequence of a different substitution of the C2 atom of the adenine derivatives L_{1-3} and L_{4-7} involved in the complexes **1**–**3** and **4**–**7**. A broad peak was observed in IR spectra of all the complexes between ca. 3300 and 3500 cm^{-1}, and thus, the maxima belonging to both the ν(N–H) and ν(O–H) vibrations could not be assigned unambiguously.

An oxalate dianion, which is bidentate-coordinated to the Pd(II) ion in complexes **1**–**7**, showed two bands of the $\nu_{as}(C{=}O)_{ox}$ vibration at 1671–1676 and 1706–1712 cm^{-1} [20]. Other peaks of an oxalato group, assignable to the $\nu_s(C–O)_{ox}$ vibration, were found in the 1364–1378 cm^{-1} region. The coordination of both ligand types to the metal centre was indirectly proved by detection of the ν(Pd–N) and ν(Pd–O) vibrations in the far-IR spectra. The bands of the ν(Pd–O) were observed at 557–560 cm^{-1}, while the maxima observed between 506 and 527 cm^{-1} are assignable to the ν(Pd–N) vibration [19–21].

Most of the above-described vibrations detected by the IR spectroscopy of **1**–**7** were observed in the corresponding Raman spectra of the complexes **2**–**7** (complex **1** burnt up in the light of laser beam). The maxima belonging to the $\nu(C–H)_{ar}$, $\nu(C–H)_{al}$, and ν(Pd–O) stretching vibrations were found in Raman spectra of all the complexes **2**–**7** at 3057–3148, 2833–2990, and at 559–561 cm^{-1}, respectively. Two maxima of the $\nu_{as}(C{=}O)_{ox}$ vibrations were detected at 1692–1711 and 1657–1672 cm^{-1}, while the maxima of the $\nu(C{=}C)_{ar}$ were observed at 1535–1549 and 1454–1485 cm^{-1}. However, the other vibrations discussed for IR spectroscopy, i.e. $\nu(C{=}N)_{ar}$, $\nu_s(C–O)_{ox}$, $\nu(C–O)_{ar}$ and ν(Pd–N), were observed only in Raman spectra of some of the palladium(II) oxalato complexes **2**–**7** (see Section 2.2). In case of the $\nu(C{=}N)_{ar}$ vibration, it could be connected with decrease in intensity of the named band, as recently experimentally observed and theoretically calculated for this vibration in adenine [18]. Nevertheless, in the cases that these bands were observed, the positions of their maxima correlated well with those observed in the IR spectra (see Section 2.2 for more details). The band of a very strong intensity at about 1320 cm^{-1}, which was not detected in the IR spectra, can be assigned to the skeletal stretching vibrations of a purine ring, as formerly reported [18,22]. Contrary to the IR spectra, the ν(N–H) bands were detected in the Raman spectra of **2**, **3**, **5** and **7** (not for **4** and **6**). However, the maxima of the peaks connected with this vibration, observed within the 3333–3370 cm^{-1} region, were of very low intensity, which is in accordance with results given for non-substituted adenine [18].

3.3. NMR spectroscopy

Multinuclear and two dimensional (2D) NMR experiments (see Section 2.3) were performed for all the complexes **1**–**7** as well as for the free organic compounds L_{1-7} involved in **1**–**7** as N-donor ligands. The chemical shifts (δ; ppm) are given in Section 2.2, while the coordination shifts ($\Delta\delta = \delta_{complex} - \delta_{ligand}$; ppm) are summarized in Tables 1–3.

All the signals detected in the ^{1}H and ^{13}C NMR spectra of the free L_{1-7} molecules were also found in the appropriate spectra of complexes **1**–**7**. The highest $|\Delta\delta|$ values in the ^{1}H NMR spectra were observed for the hydrogen atoms bound to the N^6 (0.34–0.95 ppm downfield) and C^8 (0.28–0.61 ppm downfield) atoms (see Table 1). In the case of complexes **4**–**7**, the N^{2}H signals are significantly shifted downfield as well, but less than the mentioned N^{6}H and C^{8}H signals. The coordination shifts of the other proton signals were insignificant.

The highest coordination shifts of carbon atoms were determined for the C^8 atom (3.50–3.94 ppm downfield), followed by the C^5 (1.24–3.12 ppm upfield), C^6 (0.93–2.22 ppm upfield) and C^{16} (1.31–1.75 ppm downfield) ones (Table 2). It can be pointed out, that the C^5, C^6 and C^8 coordination shifts of **1**–**3** and **4**–**7** differ significantly within the group of complexes **1**–**7**, which is most likely caused by various compositions and structures of the appropriate adenine derivatives involved in these two types of compounds. It has to be noted, that there was one more signal detected at ~166 ppm in the ^{13}C NMR spectra of the complexes **1**–**7**, which was not observed in the spectra of free L_{1-7} molecules,

Table 1
Coordination shifts ($\Delta\delta = \delta_{complex} - \delta_{ligand}$) determined from the ^{1}H NMR spectra for the complexes **1**–**7**.

	N^2H	N^6H	C^8H	C^9H	$C^{11}H$	$C^{12}H$	$C^{13}H$	$C^{14}H$	$C^{15}H$	$C^{16}H$	$C^{17}H$, $C^{18}H$	$C^{19}H$	$C^{20}H^a$	$C^{20}H^b$	$O^{20}H$	$C^{21}H^a$	$C^{21}H^b$	$C^{22}H$	$C^{23}H$	$C^{24}H$
1		0.61	0.40	0.08		0.02	−0.03	0.03	0.12	0.05	−0.05								0.04	
2		0.34	0.28	0.05	0.02		0.00	−0.03	0.07	0.01	−0.06								0.03	
3		0.52	0.47	0.07	0.07		−0.01		0.07	0.03	−0.04								0.03	0.03
4	0.46	0.71	0.61	−0.03	0.05	0.01	0.01	0.01	0.05	0.06	−0.02	−0.01	0.00	−0.07	−0.09	0.01	−0.18	−0.01		
5	0.49	0.95	0.54	0.02		0.00	0.01	−0.02	0.06	0.06	−0.03	−0.01	0.00	0.00	−0.07	0.00	−0.04	−0.01	0.01	
6	0.48	0.77	0.56	0.01	0.06		0.00	−0.02	0.06	0.07	−0.04	−0.02	−0.02	−0.03	0.06	0.00	−0.03	0.01	0.03	
7	0.49	0.76	0.55	0.01	−0.01	0.07		0.07	−0.01	0.06	−0.03	0.01	0.02	0.00	−0.01	0.02	0.00	−0.01	0.01	

Table 2
Coordination shifts ($\Delta\delta = \delta_{complex} - \delta_{ligand}$) determined from the ^{13}C NMR spectra for the complexes **1**–**7**.

	C^2	C^4	C^5	C^6	C^8	C^9	C^{10}	C^{11}	C^{12}	C^{13}	C^{14}	C^{15}	C^{16}	C^{17}	C^{18}	C^{19}	C^{20}	C^{21}	C^{22}	C^{23}	C^{24}	$C^{25,26}$
1	0.24	−0.21	−2.44	−1.09	3.77	0.92	−0.94	0.05	0.08	0.24	0.18	0.58	1.75	−0.46	−0.46					0.16		−1.38
2	0.80	−0.06	−1.24	−1.60	3.94	0.95	−0.86	−0.23	−0.03	0.43	−0.01	0.24	1.31	−0.37	−0.37					0.06		−1.23
3	0.19	−0.21	−2.37	−0.93	3.70	1.08	−1.03	0.11	0.01	0.70	0.01	0.11	1.74	−0.41	−0.41					0.12	0.12	−1.36
4	0.13	−0.42	−3.12	−2.20	3.50	0.68	−1.15	0.08	0.02	0.01	0.02	0.08	1.55	−0.54	−0.54	0.02	−0.44	−0.19	−0.10			−0.75
5	0.21	−0.28	−2.97	−2.22	3.53	0.67	−0.97	0.07	0.04	0.36	0.17	0.16	1.52	−0.51	−0.51	0.12	−0.39	−0.13	−0.03	0.12		−1.01
6	0.18	−0.34	−3.09	−2.12	3.58	0.93	−1.06	−0.36	0.13	0.61	0.06	0.17	1.54	−0.48	−0.49	0.06	−0.39	−0.15	−0.05	0.11		−0.91
7	0.20	−0.30	−3.08	−2.14	3.63	0.95	−1.18	0.07	0.23	0.06	0.23	0.07	1.63	−0.50	−0.46	0.09	−0.38	−0.13	−0.06	0.02		−0.85

Table 3
^{15}N coordination shifts ($\Delta\delta = \delta_{complex} - \delta_{ligand}$) determined from the $^{1}H–^{15}N$ gs-HMBC NMR spectra for the complexes **1**–**7**.

	N^1	N^2	N^3	N^6	N^7	N^9
1	2.7		−0.9	8.2	−93.0	7.3
2	1.5		−5.5	1.6	−98.2	1.9
3	3.6		−0.9	6.5	−92.7	6.4
4	2.0	2.6	n.o.	4.0	−96.5	6.7
5	−1.3	−1.3	−4.5	5.7	−99.0	3.7
6	−0.3	3.6	n.o.	8.8	−94.5	7.3
7	−2.8	−3.4	n.o.	12.6	−102.6	1.5

n.o. – signals were not observed in the $^{1}H–^{15}N$ gs-HMBC spectra of the appropriate complexes.

as well as in any of 2D carbon experiments. This signal unambiguously belongs to the C^{25} and C^{26} atoms of an oxalate dianion bidentate-coordinated to the metal centre. The signals of these atoms are shifted by 0.75–1.38 ppm upfield as compared with the corresponding ^{13}C NMR signal of the starting compound $K_2[Pd(ox)_2]\cdot 2H_2O$ dissolved in D_2O and detected at 166.95 ppm. As in the case of the C^5, C^6 and C^8 atoms, the $|\Delta\delta|$ of C^{25} and C^{26} are different for the complexes **1**–**3** as compared with **4**–**7**.

In the case of $^{1}H–^{15}N$ gs-HMBC 2D correlation experiments, coordination shifts of the N^7 atoms [$\Delta\delta = -92.7 - (-102.6)$ ppm] were found to be significantly higher as compared with those of the remaining nitrogen atoms ($|\Delta\delta| < 12.6$ ppm) involved in L_{1-7} molecules (Table 3). The analogical NMR spectroscopy results were recently published for palladium(II) oxalato [3] and dichlorido [5] complexes involving N6-(benzyl)-9-isopropyladenine-based N-donor ligands, whose structures were crystallographically determined. It is caused by a coordination of L_{1-7} molecules to the Pd(II) ion through the mentioned N^7 atom of the adenine moiety within the structure of the complexes **1**–**7**. In connection with this statement, we can focus back on the results of ^{1}H and ^{13}C NMR spectroscopy, where we discuss the C^8H, N^6H, C^8 and C^5 atoms as those with the highest $\Delta\delta$. As it can be seen from Schemes 1 and 2, the above-mentioned hydrogen and carbon atoms neighbour to the coordination site, i.e. the N^7 atom, which indirectly support discussed conclusion regarding coordination.

3.4. ESI+ mass spectrometry

The ESI+ MS of the complexes **1**–**7** dissolved in methanol were measured and the results are given in Section 2.2. All the observed isotopic distribution representations correspond very well with the theoretic ones (QUALBROWSER software, version 2.0.7, Thermo Fischer Scientific).

In case of the complexes **1**–**3**, involving 2-chloro-N6-(benzyl)-9-isopropyladenine-based molecules L_{1-3}, the $[Pd(ox)(L_{1-3})_2 + H]^+$ molecular peaks were found in the appropriate spectra at 858.8 *m/z* (**1**), 858.7 *m/z* (**2**) and 918.6 *m/z* (**3**), which indirectly confirmed the composition of discussed palladium(II) oxalato complexes. Moreover, the $[Pd(ox)(L_1)_2 + Na]^+$ (for **1**), $[Pd(ox)(L_1)_2 + K]^+$ (for **1**) and $[Pd(ox)(L_{1-3})_3 + H]^+$ (for **1**–**3**) adducts were observed as well. The $[Pd(ox)(L_{1-3}) + H]^+$ and $[(L_{1-3}) + H]^+$ fragments of the studied compounds were also detected in the mass spectra of **1**–**3**; $[(L_{1-3}) + H]^+$ fragment, detected at 332.1 *m/z* for **1**, 332.2 *m/z* for **2** and 362.1 *m/z* for **3**, is unambiguously assignable to the adenine derivative (L_{1-3}) involved in the structures of **1**–**3**. Fig. 1 depicts the $[Pd(ox)(L_1) + H]^+$ and $[Pd(ox)(L_1)_2 + K]^+$ peaks found in ESI+ mass spectrum of the complex **1** and their comparison with the theoretic ones.

Quite different results were obtained for the complexes **4**–**7**, since any of the $[Pd(ox)(L_{4-7})_2 + H]^+$, $[Pd(L_{5-7})_2 + H]^+$, or $[Pd(ox)(L_{4-7}) + H]^+$ peaks were not found in their mass spectra, except for $[Pd(L_4)_2 + H]^+$ observed at 813.1 *m/z*; the $[Pd(ox)(L_4)_2 + Na]^+$ and $[Pd(ox)(L_4) + Na]^+$ adducts were detected for this compound as well. On the other hand, the $[Pd(L_{4-7}) + H]^+$ fragment, whose analogue was not detected in any spectrum of **1**–**3**, was clearly observed for the compounds **4**–**7** *m/z* at 461.2, 491.1, 491.2, and 491.1, respectively. Similarly as in the case of complexes **1**–**3**, the $[Pd(ox)(L_{4-7})_3 + H]^+$ and $[(L_{4-7}) + H]^+$ peaks were found in the mass spectra of **4**–**7**.

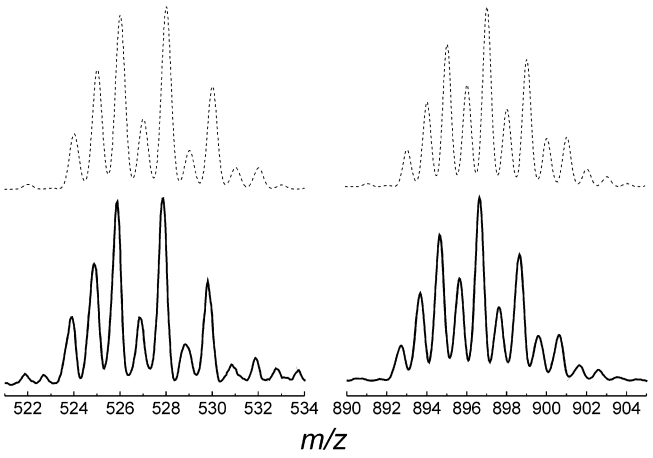

Fig. 1. Observed (full line) and calculated (dashed line) isotopic distribution representation of $[Pd(ox)(L_1) + H]^+$ (left) and $[Pd(ox)(L_1)_2 + K]^+$ (right) peaks as obtained by an ESI+ mass spectrometry of the complex **1**.

3.5. DFT calculations

The molecular structures of $[Pd(ox)(L_I)_2]$ (**I**) and $[Pd(ox)(L_{II})_2]\cdot L_{II}\cdot Me_2CO$ (**II**) complexes were determined by a single-crystal X-ray analysis, as it was reported in our previous work describing the palladium(II) oxalato complexes with N6-(benzyl)-9-isopropy-

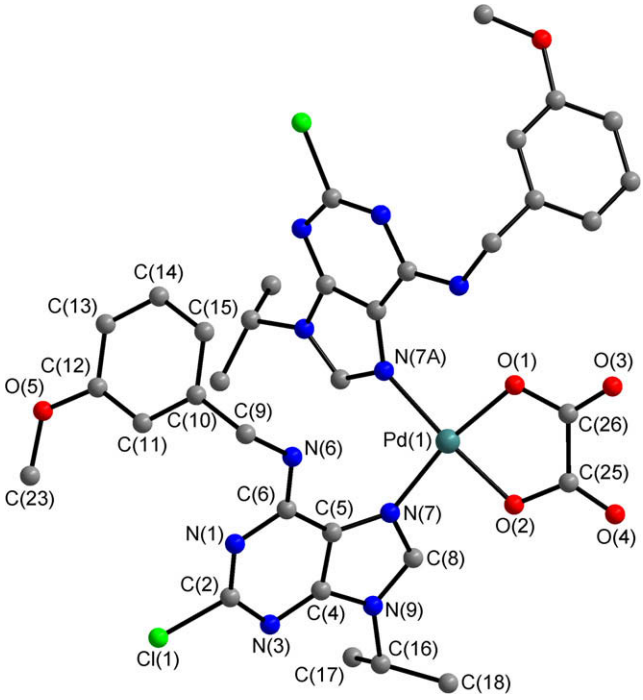

Fig. 2. Geometry of the $[Pd(ox)(L_2)_2]$ (**2**) complex optimized on the B3LYP/6-311G*/LANL2DZ level of theory.

ladenine-based N-donor ligands; L_I = 2-chloro-N6-(4-methoxybenzyl)-9-isopropyladenine, L_{II} = 2-chloro-N6-(4-methylbenzyl)-9-isopropyladenine [3]. In present work, partially due to a lack of single crystals suitable for a crystallographic study, we decided to perform theoretical calculations relating to the geometry of the complex $[Pd(ox)(L_2)_2]$ (**2**) on the B3LYP/6-311G*/LANL2DZ level, whose optimized structure is depicted in Fig. 2. The selected bond lengths and angles of the complexes **2**, **I** and **II** are given in Table 4.

The central Pd(II) ion of the complex **2** is tetra-coordinated by two 2-chloro-N6-(3-methoxybenzyl)-9-isopropyladenine (L_2) molecules bound to the metal centre through their N(7) atoms of the adenine moieties and by one bidentate-coordinated oxalate dianion. Geometry in the vicinity of the central Pd(II) ion is distorted square-planar. The deviations from a least-square plane defined by atoms of the PdN_2O_2 chromophore are: 0.027 Å for Pd(1), 0.070 Å for O(1), −0.089 Å for O(2), 0.064 Å for N(7) and −0.072 Å for N(7A). For the complex **II**, the above-discussed deviations were determined to be: 0.0005(3) Å [Pd(1)], −0.0305(22) Å [O(1)], 0.0276(27) Å [O(2)], −0.0513(29) Å [N(7)] and 0.0259(29) Å [N(7A)]. In case of the complex **II** they equalled, in the given order, 0.0032(3), −0.0202(23), −0.0643(23), −0.0530(32), and −0.1318(32) Å, respectively. Two L_2 molecules are, similarly to the complex **II**, mutually arranged in the head-to-tail arrangement within the structure of the complex **2**; the complex **I** has its L_I molecules arranged in the head-to-head orientation.

All the calculated Pd–N and Pd–O bands of **2** are slightly longer as compared with those determined for the complexes **I** and **II** (Table 4). As for bond angles, it has to be noted that in some cases [e.g. O(1)–Pd(1)–N(7)], the values observed for the complex **2** differ significantly from those of **I** and **II**. But differences of the same order can be found even between some angles of **I** and **II** [e.g. O(2)–Pd(1)–N(7A) angle], which is caused by a variedness of the structures of the studied complexes (see Table 4).

Table 4
Selected bond lengths (Å) and angles (°) for the complex $[Pd(ox)(L_2)_2]$ (**2**) optimized on the B3LYP/6-311G* /LANL2DZ level of theory, and for the complexes $[Pd(ox)(L_I)_2]$ (**I**) and $[Pd(ox)(L_{II})_2]\cdot L_{II}\cdot Me_2CO$ (**II**) as determined by a single-crystal X-ray analysis (see Ref. [3]); L_2 = 2-chloro-N6-(3-methoxybenzyl)-9-isopropyladenine, L_I = 2-chloro-N6-(4-methoxy-benzyl)-9-isopropyladenine and L_{II} = 2-chloro-N6-(4-methylbenzyl)-9-isopropyladenine.

Compound	2	I	II
Bond lengths			
Pd(1)–N(7)	2.078	2.012(3)	2.023(3)
Pd(1)–N(7A)	2.110	2.024(3)	2.021(3)
Pd(1)–O(1)	2.017	1.992(2)	1.971(2)
Pd(1)–O(2)	2.011	1.987(2)	1.983(2)
O(1)–C(26)	1.355	1.302(4)	1.332(4)
O(2)–C(25)	1.351	1.289(4)	1.282(4)
O(3)–C(26)	1.234	1.215(4)	1.239(4)
O(4)–C(25)	1.233	1.222(4)	1.230(4)
C(25)–C(26)	1.540	1.549(5)	1.471(5)
Bond angles			
O(1)–Pd(1)–N(7A)	95.37	93.09(10)	89.86(10)
O(1)–Pd(1)–N(7)	168.73	174.96(10)	173.26(10)
O(1)–Pd(1)–O(2)	82.28	84.46(9)	84.20(10)
O(2)–Pd(1)–N(7)	86.83	91.12(10)	89.38(10)
O(2)–Pd(1)–N(7A)	173.54	177.10(10)	171.75(10)
N(7)–Pd(1)–N(7A)	95.76	91.39(11)	96.32(11)
Pd(1)–O(1)–C(26)	114.48	111.8(2)	110.6(2)
Pd(1)–O(2)–C(25)	114.67	111.8(2)	111.5(2)
O(1)–C(26)–O(3)	122.62	125.2(3)	121.1(3)
O(2)–C(25)–O(4)	123.38	124.9(3)	123.0(3)
O(1)–C(26)–C(25)	114.02	115.3(3)	116.3(3)
O(2)–C(25)–C(26)	114.33	115.9(3)	117.4(3)
O(3)–C(26)–C(25)	123.36	119.5(3)	122.5(3)
O(4)–C(25)–C(26)	122.30	119.3(3)	119.6(3)
Pd(1)–N(7)–C(5)	134.37	127.9(2)	135.8(2)
Pd(1)–N(7)–C(8)	118.18	126.9(2)	119.2(2)
C(5)–N(7)–C(8)	106.45	105.2(3)	105.0(3)
Pd(1)–N(7A)–C(5A)	134.31	129.8(2)	129.9(2)
Pd(1)–N(7A)–C(8A)	119.50	124.8(2)	119.6(2)
C(5A)–N(7A)–C(8A)	106.11	105.4(3)	105.3(3)

3.6. Thermal analysis

The TG and DTA methods of a thermal analysis of **1**–**7** indicated two types of thermal behaviour of the complexes **1**–**3** and **4**–**7**. As representatives of both groups, the complexes **3** and **4** were chosen for detailed interpretation and their TG/DTA curves are depicted in Fig. 3. All the important thermal characteristics of the studied complexes are given in Table 5.

The dehydration of **3** began right after the start of the analysis at 28 °C, and this first step is finished at 132 °C. The endothermic effects (*endo*-effects), anticipated for the dehydration process, were found on the DTA curve with minima at 40 and 124 °C. The compound existed in its dehydrated form of $[Pd(ox)(L_3)_2]$ between 132 and 149 °C. Consequently, the decay proceeded in three waves without formation of thermally stable intermediates up to 480 °C. This process is accompanied by two exothermic effects (*exo*-effects) on the DTA curve (Table 5) with maxima at 182, and 368 °C, respectively. A plateau, which may be connected with the formation of a thermally stable intermediate palladium(II) oxide (PdO), occurred on the TG curve from 480 up to 808 °C. The PdO further decomposed to Pd (with the minimum of *endo*-effect at 816 °C), which formed as a final product of the thermal degradation of **3**. No weight changes were observed on the TG curve from 820 °C to the final temperature of the experiment (900 °C). The observed weight losses of described partial processes of the thermal decomposition of **3** differ insignificantly from the calculated ones (Table 5).

The anhydrous complex $[Pd(ox)(L_3)_2]$ (**4**) is thermally stable up to 128 °C (Fig. 3). The process of thermal degradation proceeded from this temperature, with three steps observable on the TG curve, without formation of any thermally stable intermediates up to 544 °C, when it is finished by a formation of PdO. As it is given in Table 5, four *exo*-effects and two *endo*-effects were detected on the DTA curve in connection with this process. The second weak *endo*-effect, whose minimum is lying at 163 °C, is most likely connected with melting and simultaneous decomposition of the complex **4** (melting temperature determined by a melting point apparatus was found to be 164–166 °C). The PdO was thermally stable in the 544–803 °C range. Its decomposition to Pd was observed at 803–837 °C and it was accompanied by *endo*-effect on

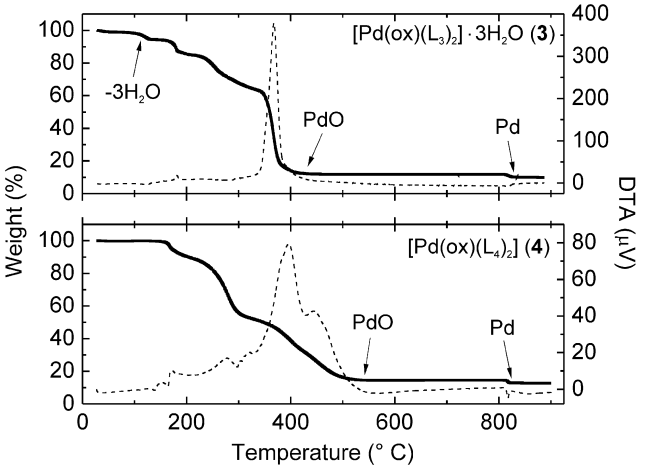

Fig. 3. TG/DTA curves of the complexes **3** and **4** as obtained in the dynamic air atmosphere in the 25–900 °C temperature range.

Table 5
Results of TG/DTA thermal analyses of the palladium(II) oxalato complexes **1**–**7**.

Complex	Dehydration		$[Pd(ox)(L_n)_2]$	$[Pd(ox)(L_{1-7})_2] \rightarrow PdO$		PdO	$PdO \rightarrow Pd$		DTA (°C)[d]	
	T (°C)[a]	Δm (%)[b]	T (°C)[c]	T (°C)[a]	Δm (%)[b]	T (°C)[c]	T (°C)[a]	Δm (%)[b]	*endo*-effect	*exo*-effect
$[Pd(ox)(L_1)_2]\cdot{}^3/_4H_2O$ (**1**)	61–149	1.6/1.6		149–445	84.4/83.5	445–816	816–845	1.8/1.8	828	171, 416
$[Pd(ox)(L_2)_2]\cdot{}^3/_4H_2O$ (**2**)	28–145	1.6/1.5		145–475	84.4/83.5	475–821	821–851	1.8/1.6	824	178, 419
$[Pd(ox)(L_3)_2]\cdot 3H_2O$ (**3**)	28–145	5.6/5.7	132–149	145–480	81.9/82.5	480–808	808–835	1.6/1.6	40, 124, 816	182, 368
$[Pd(ox)(L_4)_2]$ (**4**)			29–128	128–544	86.5/85.3	544–803	803–837	1.8/1.6	138, 163, 817	170, 278, 396, 444
$[Pd(ox)(L_5)_2]$ (**5**)			30–109	109–569	87.3/86.0	569–809	809–831	1.7/1.7	158, 823	170, 301, 353, 407
$[Pd(ox)(L_6)_2]\cdot H_2O$ (**6**)	28–130	1.8/1.6		130–578	85.7/85.4	578–806	806–821	1.7/1.7	156, 815	173, 300, 429
$[Pd(ox)(L_7)_2]$ (**7**)			28–133	133–552	87.3/85.9	552–811	811–836	1.7/1.6	164, 825	172, 287, 411

[a] The temperature range of the corresponding transformation process.
[b] Weight losses; calcd./found.
[c] The temperature range of a thermally stable intermediate.
[d] Positions of minima of endothermic effects (*endo*-effect) and maxima of exothermic effects (*exo*-effect).

the DTA curve with a minimum at 817 °C. A plateau of thermally stable palladium can be seen above 837 °C to the final temperature of 900 °C. Again, the obtained and calculated weight losses correlated well with each other (see Table 5).

3.7. In vitro cytotoxicity

Promising *in vitro* cytotoxicity (tested by an AM assay) results of several palladium(II) oxalato complexes with 2-chloro-N6-(benzyl)-9-isopropyladenine-based derivatives against K562 and MCF-7 human cancer cell lines were reported in our previous paper [3]. That is why we decided to test several representatives (namely the complexes **1**, **3**–**5** and **7**) of a new series of palladium(II) oxalato complexes involving mentioned N-donor ligands. However, an MTT assay was used instead of an AM one, which reduces comparability of both groups of results.

The tested complexes showed the following *in vitro* cytotoxic activities against HOS cancer cells: >50.0 μM for **1**, >5.0 μM for **3**, >25.0 μM for **4**, 34.9 ± 11.0 μM for **5**, and 39.2 ± 6.0 μM for **7**. The obtained values were compared with that of platinum-based anticancer drug *Cisplatin*, whose IC_{50} value was found to be 34.2 ± 6.4 μM, as determined by an MTT test. It can be seen that *in vitro* cytotoxicity of tested complexes **5** and **7** is comparable with that of *Cisplatin*. The results presented herein as well as in our previous paper [3] encourage us to continue with the biological testing and to test these complexes by an MTT assay for their *in vitro* cytotoxicity against some other human cancer cell lines, which is currently in progress. Moreover, the DNA interaction study, as well as the *in vivo* testing will be carried out for the palladium(II) oxalato complexes involving N6-(benzyl)-9-isopropyladenine-based derivatives in the near future.

4. Conclusions

A series of $[Pd(ox)(L_{1-7})_2]\cdot nH_2O$ (**1**–**7**; n = 0 for **4**, **5** and **7**, ¾ for **1** and **2**, 1 for **6** and 3 for **3**) palladium(II) oxalato complexes was synthesized by reactions of $K_2[Pd(ox)_2]\cdot 2H_2O$ with two molar equivalents of the appropriate L_{1-7} organic compound. The pale yellow powder products were isolated in good yields and characterized by various physical methods. Within the complexes **1**–**7**, compounds **1**–**3** represent analogues of recently published palladium(II) oxalato complexes with 2-chloro-N6-(benzyl)-9-isopropyladenine derivatives [3] similar to L_{1-3} molecules, but with differently substituted benzyl group. On the other hand, we report here the substances **4**–**7** as the first palladium(II) oxalato complexes involving the highly potent CDK inhibitors, namely 2-(1-ethyl-2-hydroxyethylamnio)-N6-(benzyl)-9-isopropyladenine (*Roscovitine*; L_4) or its analogues with the substituted benzyl group (L_{5-7}), as N-donor carrier ligands.

Based on the obtained results, the complexes **1**–**7** have been characterized as square–planar compounds with the central Pd(II) ion tetra-coordinated by one bidentate O-donor oxalate dianion and two adenine derivatives bound to the metal centre through N7 atoms of their adenine moieties, thus giving a PdN_2O_2 chromophore. The prepared complexes **1**, **3**–**5** and **7** were tested *in vitro* for their antitumour activity against human osteosarcoma cancer cell line, HOS. The obtained results showed the complexes **5** and **7** as the substances with *in vitro* cytotoxicity comparable with commercially used platinum-based drug *Cisplatin*.

Acknowledgements

The financial support from the Ministry of Education, Youth and Sports of the Czech Republic is gratefully acknowledged (a Grant No. MSM6198959218). The authors also thank Mrs. Pavla Richterová for performing CHN elemental analyses, Ms. Radka Novotná for infrared and Raman spectra measurements, Ms. Alena Klanicová for mass spectra measurements and Dr. Radim Vrzal and Prof. Zdeněk Dvořák for *in vitro* cytotoxicity testing.

Appendix A. Supplementary material

A scheme of the synthetic pathway of L_{1-7} organic compounds, as well as their IR, Raman and NMR (^1H, ^{13}C, ^{15}N) spectral data, are deposited. Supplementary data associated with this article can be found, in the online version, at doi:10.1016/j.ica.2010.01.035.

References

[1] P.J. Davies, Plant Hormones, 3rd ed., Springer, Dordrecht, 1997.
[2] M. Gielen, E.R.T. Tiekink, Metallotherapeutic Drugs and Metal-based Diagnostic Agents, Willey, London, 2005.
[3] P. Štarha, Z. Trávníček, I. Popa, J. Inorg. Biochem. 103 (2009) 978.
[4] A. Garoufis, S.K. Hadjikakou, N. Hadjiliadis, Coord. Chem. Rev. 253 (2008) 1384.
[5] Z. Trávníček, L. Szüčová, I. Popa, J. Inorg. Biochem. 101 (2007) 477.
[6] K.I. Lee, T. Tashiro, M. Noji, Chem. Pharm. Bull. 42 (1994) 702.
[7] L. Meijer, A. Borgne, O. Mulner, J.P.J. Chong, J.J. Blow, N. Inagaki, M. Inagaki, J.G. Delcros, J.P. Moulinoux, Eur. J. Biochem. 243 (1997) 527.
[8] K. Torigoe, K. Esumi, Langmuir 9 (1993) 1664.
[9] M. Legraverend, O. Ludwig, E. Bisagni, S. Leclerc, L. Meijer, N. Giocanti, R. Sadri, V. Favaudon, Bioorg. Med. Chem. 7 (1999) 1281.
[10] C.H. Oh, S.C. Lee, K.S. Lee, E.R. Woo, C.Y. Hong, B.S. Yang, D.J. Baek, J.H. Cho, Arch. Pharm. Pharm. Med. Chem. 332 (1999) 187.
[11] J.W. Daly, B.E. Christensen, J. Org. Chem. 21 (1956) 177.
[12] P. Imbach, H.G. Capraro, P. Furet, H. Mett, T. Meyer, J. Zimmermann, Bioorg. Med. Chem. Lett. 9 (1999) 91.
[13] SPARTAN06 (Version 1.1.2), Wavefunction Inc., 18401 Von Karman Avenue, Suite 370, Irvine, CA 92612, USA.
[14] K. Brandenburg, DIAMOND, Release 3.1f, Crystal Impact GbR, Bonn, Germany, 2006.
[15] J. Ulrichová, Z. Dvořák, J. Vičar, J. Lata, J. Smržová, A. Šedo, V. Šimánek, Toxicol. Lett. 125 (2001) 125.

[16] W.J. Geary, Coord. Chem. Rev. 7 (1971) 81.
[17] C.J. Pouchert, The Aldrich Library of Infrared Spectra, 3rd ed., Aldrich Chemical Co., Milwaukee, 1981.
[18] T.A. Mohamed, I.A. Shabaan, W.M. Zoghaib, J. Husband, R.S. Farag, A.E.M.A. Alajhaz, J. Mol. Struct. 938 (2009) 263.
[19] V. Montoya, J. Pons, J. García-Antón, X. Solans, M. Font-Bardia, J. Ros, Inorg. Chim. Acta 360 (2007) 625.
[20] K. Nakamoto, Infrared and Raman Spectra of Inorganic and Coordination Compounds, 5th ed., Willey-Interscience, New York, 1997.
[21] M. Espinal, J. Pons, J. García-Antón, X. Solans, M. Font-Bardia, J. Ros, Inorg. Chim. Acta 361 (2008) 2648.
[22] Z. Dhaouadi, M. Ghomi, J.C. Austin, R.B. Girling, R.E. Hester, P. Mojzes, L. Chinsky, P.Y. Turpin, C. Coulombeau, H. Jobic, J. Tomkinson, J. Phys. Chem. 97 (1993) 1074.